2

AAEC/E432

AAEC/E432

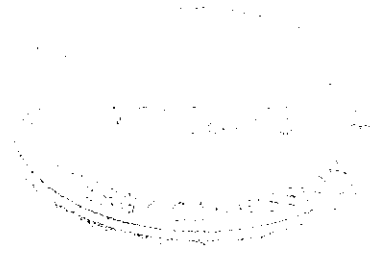

AUSTRALIAN ATOMIC ENERGY COMMISSION

RESEARCH ESTABLISHMENT

LUCAS HEIGHTS

MONTE CARLO CALCULATIONS OF TIME-DEPENDENT NEPTUNIUM-237 AND URANIUM-235 FISSION RATES IN A PULSED THORIUM ASSEMBLY

by

B.J. McGREGOR

November 1977

ISBN 0 642 59631 X

AUSTRALIAN ATOMIC ENERGY COMMISSION

RESEARCH ESTABLISHMENT

LUCAS HEIGHTS

MONTE CARLO CALCULATIONS OF TIME-DEPENDENT NEPTUNIUM-237 AND URANIUM-235 FISSION RATES IN A PULSED THORIUM ASSEMBLY

by

B. J. McGREGOR

ABSTRACT

A series of integral pulsed neutron experiments in a thorium assembly have been performed. Monte Carlo calculations are presented of the ^{237}Np and ^{235}U fission rates as a function of space and time. Calculations assuming spherical symmetry are compared with those which represent the geometry of the experiment nearly exactly, and both are compared with the experimental results. It is shown that the calculations give similar results for the simplified and actual geometries. It is concluded that the observed differences between calculation and experiment are not due to errors in the calculations introduced by the use of simplifying geometric assumptions.

National Library of Australia card number and ISBN 0 642 59631 X

The following descriptors have been selected from the INIS Thesaurus to describe the subject content of this report for information retrieval purposes. For further details please refer to IAEA-INIS-12 (INIS: Manual for Indexing) and IAEA-INIS-13 (INIS: Thesaurus) published in Vienna by the International Atomic Energy Agency.

MONTE CARLO METHOD; FISSION; NEPTUNIUM 237; URANIUM 235; PULSED NEUTRON TECHNIQUES; CROSS SECTIONS; THORIUM 232

CONTENTS

		Page
1.	INTRODUCTION	1
2.	CALCULATIONAL METHOD	2
2.1	'Symmetric' and 'Asymmetric' Calculations	2
2.2	Energy and Time Dependence of the Source	2
2.3	Angular Dependence of the Source	2
2.4	Cross Sections	2
2.5	Fission in ^{232}Th	2
3.	MONTE CARLO CALCULATIONS	3
3.1	Normalisation of Calculation and Experiment	3
3.2	Processing of Results	4
4.	COMPARISON OF MONTE CARLO CALCULATIONS WITH EXPERIMENT	5
5.	DISCUSSION	5
5.1	Asymmetric and Transport Corrected Symmetric Calculations	5
5.2	Consistent *vs* Transport Corrected Symmetric Calculations	7
5.3	Summary of ^{235}U Results	8
5.4	^{237}Np Results	9
6.	SUMMARY	9
7.	ACKNOWLEDGEMENTS	10
8.	REFERENCES	10
TABLE 1	Group-Dependent Quantities	11
Figure 1	Theoretical and experimental values of the fundamental mode fission rates for ^{237}Np as a function of time (a) The fundamental mode time distribution (b) The instantaneous decay constant $\lambda(t)$	13
Figure 2	Theoretical and experimental values of the fundamental mode fission rates for ^{235}U as a function of time (a) The fundamental mode time distribution (b) The instantaneous decay constant $\lambda(t)$	14
Figure 3	Angle-integrated neutron energy spectrum from the $^{9}Be(d,n)\ ^{10}B$ thick target reaction	15
Figure 4	Angular distributions of fast neutron fluence produced by unit current of deuteron beam incident on a thick Be disk at various bombarding energies	16
Figure 5	Comparison of asymmetric and transport symmetric calculations with experimental ^{235}U fission rate at 4 positions	17

(continued)

CONTENTS (continued)

		Page
Figure 6	Comparison of averaged asymmetric and transport symmetric calculations with averaged experimental ^{235}U fission rate at 4 positions	18
Figure 7	Comparison of symmetric P3 and transport symmetric calculations with averaged experimental ^{235}U fission rate at 4 positions	19
Figure 8	Comparison of consistent and transport symmetric calculations with averaged experimental ^{235}U fission rate at 4 positions	20
Figure 9	Comparison of asymmetric and transport symmetric calculations with experimental ^{237}Np fission rate at 4 positions	21
Figure 10	Comparison of averaged asymmetric and transport symmetric calculations with averaged experimental ^{237}Np fission rate at 4 positions	22
Figure 11	Comparison of consistent and transport symmetric calculations with averaged experimental ^{237}Np fission rate at 4 positions	23
Figure 12	Target geometry	24

1. INTRODUCTION

A series of integral pulsed neutron experiments in a thorium assembly have been performed at the AAEC Research Establishment [Moo, Rainbow & Ritchie 1973]. The experiments consisted of measuring the space-dependent, time-dependent fission rates of ^{237}Np, ^{235}U and ^{239}Pu following the injection of a short burst of fast neutrons into the centre of the assembly which was a cube of about 0.4 m side. Analysis of the data was directed mainly to the extraction of the fission rates corresponding to the fundamental three-dimensional Fourier spatial mode.

A further paper [Moo, Rainbow & Ritchie 1974] compared these experimental fundamental mode fission rates with fission rates calculated with the diffusion theory code TENDS (Maher, Ritchie & Rainbow 1967] which uses asymptotic reactor theory to describe leakage. Three different thorium cross section sets derived from the ABBN set, the UKAEA Nuclear Data Library (UKNDL68) file and the ENDF/B-II file were used in those calculations and the results compared with each other and with experiments. The results of Moo *et al.** are re-presented here in Figures 1 and 2 which show the ^{237}Np and ^{235}U reaction rates with the fundamental mode. They* also derived the 'instantaneous decay constant', $\lambda(t)$. For the ^{237}Np case, they found that, near the peak of the time distributions, all combinations of ^{232}Th data sets and ^{237}Np fission cross section sets predict a faster rate of decay than was measured in the experiment. Away from the peak, the measured fundamental mode and the associated $\lambda(t)$ lie within the calculated curves.

They also found that the calculated ^{235}U fission rates using various combinations of ^{232}Th data and ^{235}U fission cross section sets are in close agreement. All three ^{232}Th data sets predict too fast a decay rate for the ^{235}U fission rate compared to measurements for the first 80 ns or so, after the peak; at later times, the predicted values of $\lambda(t)$ are close to the measured values.

A possible cause of the discrepancies between experiment and their calculations was the inadequacy of space-independent diffusion theory to handle the calculation at early times. Another possible problem was the use of a combination of Fourier modes with boundary conditions at the extrapolated boundary to represent a situation at early times where the neutrons cannot have travelled far from the source. In this study, the experiment has been examined with the Monte Carlo method. This potentially more accurate method should remove uncertainties in the theoretical calculations. Comparisons are made with the experimentally measured fission reaction rates as a function of position and time.

*Moo, Rainbow & Ritchie, 1974

2. CALCULATIONAL METHOD

2.1 'Symmetric' and 'Asymmetric' Calculations

Two types of Monte Carlo calculations were performed which will simply be called 'symmetric' and 'asymmetric'. For the symmetric calculations, the source was assumed spherically symmetric at the centre of a homogeneous sphere with an equivalent radius. Detectors were spherical shells at the same radius as the source-detector distance in the experiment. Scattering was treated in the P0 approximation both with consistent and transport-corrected total cross sections. For the asymmetric calculations, the angular dependence of the source was included, the geometry was cubic with the source hole included, and detectors were represented as cylindrical shells of the same length and orientation as those in the experiments. Scattering was treated in the P3 approximation. The target, its copper backing and surrounding brass nut were included in the geometry representation.

2.2 Energy and Time Dependence of the Source

The energy dependence of the source was assumed to be the same as in the previous calculations. Above 200 keV, the $^{9}Be(d,n)^{10}B$ neutron spectrum was obtained by integrating the angle-dependent neutron spectra measurements of Inada, Kawachi and Hiramoto [1968]. This neutron spectrum is shown in Figure 3. The spectrum was assumed to be flat from 15 to 200 keV. The time behaviour of the source was assumed to be Gaussian with the same full width at half mean height (FWHM) as that of the beam pulse measured during the experiments.

2.3 Angular Dependence of the Source

For the asymmetric calculations, the angle-dependent measurements previously quoted were sampled. The measurements integrated over outgoing neutron energies are reproduced in Figure 4 for the deuteron energy of 2.8 MeV.

2.4 Cross Sections

The same 50-group structure used in the previous calculations was employed. Thorium data were obtained from the ENDF/B-III file using SUPERTOG [Wright *et al.* 1969]. The ^{237}Np and ^{235}U fission cross sections were those taken previously from ENDF/B-II. There are apparently no differences between the version II and III ^{232}Th data sets.

2.5 Fission in ^{232}Th

High energy fissions in ^{232}Th add about 8 per cent to the neutron production. The shape of the time distribution for fission production is somewhat broader and peaks later than the initial neutron spectra. The differences between the spectra were not sufficient to show any noticeable differences

between normalised calculations with and without fission. The effects of fission in ^{232}Th were not included, as the increased neutron production due to fission was accounted for in the normalisation of the calculations to the experiment.

3. MONTE CARLO CALCULATIONS

The combinatorial geometry version of MORSE [Emmett 1975] was used for the Monte Carlo calculations.

For the symmetric calculations, a radius of 24.9 cm was assumed and the fluxes and fission reaction rates were calculated at four radial shells corresponding to the positions X = 0, 5, 10, 15 cm in scan hole A of the experiment. This is a hole parallel to the source beam (X direction) and situated 8.24 cm from the centre.

A boundary-crossing estimator was used at these positions with the microscopic fission cross sections as response functions. Forty five thousand source neutrons were treated in a three-hour run on an IBM360/50 computer. The fission reaction rate and associated errors were determined for 128 time bins (2.49 ns wide) and punched on cards using a modified subroutine ENDRUN.

The source routine for asymmetric runs included sampling for the angular dependence of the source. The seven detector surfaces were parts of the cylindrical shell of radius 8.24 cm. They were 2.54 cm in length and centred at the positions 0, ± 5, ± 10 and ± 15 cm. With the smaller detector surface area, about 170,000 source neutrons were analysed in two six-hour runs on the computer to obtain statistics still markedly worse than those obtained for the symmetric case. Separate runs were required to calculate the ^{237}Np and ^{235}U reaction rates because of the different width of the source distribution in the two cases.

3.1 Normalisation of Calculation and Experiment

No experimental information is available to indicate either the number of source neutrons, or the time at which they are emitted relative to the time channel information collected. Detector efficiencies are also unknown. The calculations need to be normalised to the experiment in two ways. The time normalisation is fairly straightforward since both calculation and experiment have well defined peaks and the calculations are assumed to peak at the same channel as the experiment.

The normalisation for the number of source neutrons and detector efficiencies is not as straightforward. As a first attempt, the results at X = 0 (90° to beam direction) were used and the peak heights equated in the calcula-

tion and experiment to give a normalisation factor for the calculations at every detector. However, this made the normalisation depend on the accuracy of the proportion of source neutrons emitted at 90° to the source direction. Since the peak of the time distribution occurs only 8 ns after the peak in the source pulse, the peak has a high proportion of uncollided and singly collided neutrons emitted at near 90° angles.

The second attempt at normalisation was to sum up the reaction rate for the seven detectors and equate the peak height to that obtained by summing the seven corresponding experimental reaction rates. In this way, the effects of any errors in the asymmetry of the source would be reduced.

Another scheme was to normalise so that the calculation and experiment were approximately equal at long times, either by fitting or hand adjustment of the normalisation factor. Finally, the calculations could be Fourier analysed and the peak of the fundamental mode equated to that obtained from a similar analysis of the experiment.

The 'best' choice of a place to normalise would be where it is known, by some means, that calculation and experiments agree. Such a place is not known.

It was decided to normalise at the peak of the time distributions, and the second method involving a summation over detectors in the forward and backward direction was used. For each calculation, the peak of the sum of the seven detector reaction rates is equated to the sum of the corresponding experimental rates multiplied by the appropriate normalisation factor.

3.2 Processing of Results

A program was written to produce plotted comparisons of calculation and experiment. The timing jitter correction was first applied. This was assumed to be Gaussian in shape with a standard deviation of 4.15 ns for both ^{237}Np and ^{235}U. This correction has the effect of slightly broadening and delaying the initial peak. The required normalisation factor was next obtained together with the required channel shift to make the peak in the calculation and experiment fall at the same channel.

To decrease the statistical uncertainty of the Monte Carlo results, especially those from the asymmetric calculations, the results in adjacent time channels were combined. The first six channels were left unchanged, the next twelve were combined into six sets of two, the next sixteen into four sets of four, and then every eight consecutive channels were combined. Results were then plotted against the experimental measurements for each detector. The processing program has an option to combine two computer runs together and to compare two calculations.

4. COMPARISON OF MONTE CARLO CALCULATIONS WITH EXPERIMENT

Figure 5 shows a comparison of the asymmetric and transport corrected symmetric calculations with the experimental results for the ^{235}U reaction rate at the seven detector positions in scan hole A corresponding to X = 0, ±5, ±10 and ±15. The normalisation factors on these calculations are 0.543 for the asymmetric calculations and 0.541 for the transport corrected symmetric calculation. To allow easy visual comparison in Figures 5-11, the results at 0 are multiplied by 9, those at ±5 by 3 and those at ±15 by $\frac{1}{3}$. The upper curves and points for each distance are for the forward direction, whereas the lower results are for the backward direction.

Figure 6 shows averages of the forward and backward results of the data given in Figure 5. Figure 7 shows a comparison of a calculation with a symmetric source and P3 scattering with the transport corrected symmetric calculations and experiment.

Figure 8 is a comparison of transport corrected and consistent symmetric calculations with the experimental results for the ^{235}U reaction rate, again at four positions, 0, ±5, ±10 and ±15. Normalisation factors are 0.507 for the consistent symmetric, and 0.541 for the transport corrected symmetric calculation.

Figure 9 compares asymmetric and transport corrected symmetric calculations with the experimental results for the ^{237}Np reaction rate at seven detector positions. Normalisation factors are 0.146 for the asymmetric and 0.147 for the transport corrected symmetric calculation. Figure 10 compares the averaged results from Figure 9. Figure 11 compares the consistent and transport corrected symmetric calculations for the ^{237}Np reaction rate.

5. DISCUSSION

5.1 Asymmetric and Transport Corrected Symmetric Calculations

In Figure 5, we can examine the comparison of transport corrected symmetric calculation with the asymmetric calculation and experiment for ^{235}U. The transport corrected symmetric calculations are the closest approximation to the previous calculations. They differ from them in being one-dimensional transport rather than zero-dimensional diffusion calculations. The asymmetric calculations are the closest representation of the experiment, and the immediate question to be examined in Figure 5 is whether this calculation fits the experiment better than the appropriate transport corrected symmetric calculation.

Considering the top curves in Figure 5 (^{235}U-X=0 position, normal to beam direction), the comparisons between calculation and experiment have sim-

ilar features to those given for previous fundamental mode calculations in Figure 1. Both calculated curves decrease more sharply than the experiment from the peak to channel 40 (∿ 100 ns). They are then nearly parallel to, although tending to diverge slightly further from, the experimental reaction rate. With the normalisation used, the asymmetric calculation tends to be ∿ 10 per cent lower than the transport corrected symmetric calculation, except for channels 13 to 20 where they are in agreement. If further normalisation factors of ∿ 1.3 for the symmetric case and ∿ 1.4 for the asymmetric case were applied, the calculations and experiment would be in good agreement except near the peak, with the asymmetric results giving better agreement near the peak.

Similar comments are true for the comparisons at ±5 cm (the second set of curves). At these detectors, there is only a small difference, even at the peak, in the experimental results for the forward and backward directions. When the detectors are at ±10 cm (the third set of curves) it is evident that the asymmetric calculation is too high in the forward direction and too low in the backward direction. At the peak, the ratio of the results in the forward and backward direction is 1.5, whereas the experimental ratio is ∿ 1.3. An initial series of calculations did not include the target geometry (Figure 12). The beryllium target and copper backing scatter neutrons are emitted in the forward direction only, and hence they remove some of the effect of the source asymmetry. With a void in the target area, the ratio near the peaks of the results at +10 divided by those at -10 was ∿ 2.0. Inclusion of the target also produces a slight broadening of the peaks.

At long times, when the effects of asymmetry have died out, the comparisons are similar to those for X=0, ± 5. With the detectors at ± 15 (bottom set of curves), the ratio of the calculated peaks in the forward and backward directions is ∿ 2.2, whereas the experimental ratio is ∿ 1.5. Beyond channel 50, the results are similar to those from the other detectors.

A general feature of the comparisons in Figure 5 is that the calculated peaks are sharper than those measured. The broader experimental peak could be caused by neutrons at the peak having undergone more collisions than the calculations indicate. The shapes of the calculated response at detectors in the backward direction (at -10 and -15) are similar to the experimental shapes.

The peaks in the calculated responses occur at approximately twice the time it would take neutrons at the peak of the source distribution to reach the particular detector. The time is slightly less in the forward and greater in the backward direction.

Reasons for the discrepancy in peak shape are unknown. A much larger timing jitter correction or a much longer source distribution would explain it, but the size of these effects is considered to be well determined.

The asymmetric calculations are too asymmetric, being high in the forward and low in the backward direction when compared to the experiment near the peak. If the calculations are giving a peak owing to neutrons with markedly fewer collisions, this effect would be expected to occur to some degree. A further possible explanation is that surface oxidation of the target may have reduced the effective deuteron energy to a value with a less asymmetric spectrum. To check that the measured angular distribution was being reproduced, a sample of 10,000 source neutrons was compared with the required distribution in Figure 4, with good agreement.

Figure 6 allows a comparison to be made of the agreement between the asymmetric and transport corrected symmetric calculations as a function of distance along scan hole A. The effects of asymmetry are removed by averaging both the asymmetric calculations and the experimental results on either side of the source. This representation makes some of the features noticed in Figure 5 readily apparent. Near the peak, the averaged asymmetric calculation agrees with the averaged experiment better than the transport symmetric calculation, which is too high at X = 0 and then steadily decreases as X increases. At long times (> 100 ns), the asymmetric results are definitely less than the transport symmetric and they are probably diverging further from the experiment, but the statistical uncertainties are such that they could be considered parallel.

5.2 Consistent *vs* Transport Corrected Symmetric Calculations

The consistent calculations use the P0 scattering cross sections without alteration with symmetric source and detector geometry. The transport correction is to subtract the total of the P1 transfers from the P0 total cross section (actually one third of the ANISN P1 component is subtracted since it has already been multiplied by three). The correction is quite substantial, the initial average mean free path of source neutrons being 7.4 cm with the transport correction, compared to 4.7 cm for the consistent set.

Figure 8 (top curves) is a comparison at X = 0 of the ^{235}U fission rate from the consistent and transport corrected symmetric calculations. The two calculations are nearly in agreement near the peak, both being higher than the experiment. The consistent results have a six per cent lower normalisation factor than the transport results. Beyond the peak, the consistent symmetric calculation is in good agreement with the experiment. For X = 5,

the consistent calculation is in good agreement with the experiment at all times. For X = ±10 both the consistent and transport corrected calculations are low at the peak, but the consistent calculation agrees with the experiment at later times. For X = ±15, the differences at the peak are increased, but the consistent calculation tends to agreement with the experiment at long times.

5.3 Summary of ^{235}U Results

Peak reaction rate

In general, the asymmetric calculations give a reasonable prediction of the difference in the peak reaction rates in the forward and backward directions. When the forward and backward results are averaged and compared with similarly averaged experimental results (Figure 6), the asymmetric results are in good agreement with the experiments at the peak for all four distances. The transport corrected and consistent calculations are themselves in agreement near the peak, but are higher than the experiment at X = 0 and get less than the experiment as X increases. This variation with distance is not present in the asymmetric P3 calculations. The most accurate calculation of the experiment at and near the peak would seem to require the inclusion of both the source asymmetry and a P3 scattering approximation. In Figure 7 a comparison is made between a symmetric source with P3 scattering calculation, and one with transport corrected P0 symmetric calculation. The variation between the two calculations near the peak in Figure 7 is about half that observed in Figure 6.

Intermediate times 30-100 ns (channel 12-40)

Compared to the experiment, both the asymmetric and transport corrected symmetric calculations decrease smoothly and are lower than the experiment at channel 40, the difference tending to increase as X increases and the asymmetric results at channel 40 being lower than the transport symmetric results. The consistent symmetric results are in agreement with the experiment by channel 40.

Long times > 100 ns

The consistent and transport corrected symmetric results are parallel to the experiment, while the asymmetric results tend to diverge slightly away from the experiment.

Transport corrected or consistent calculations

It seems that the consistent calculations are in much better agreement with the experiment. The transport approximation itself is an empirical approach which only has a theoretical backing when the flux shape settles

into its asymptotic mode. The use of this approximation at early times could be inappropriate. It is at these early times that the transport correction is a significant part of the total cross section. Alternatively, the normalisation factors on the transport corrected calculations could be determined by the fit to the experiment at long times when the transport approximation is appropriate. The fact that the calculations would then be much higher than the experiment near the peak, especially for low X values, could be explained by the transport correction being too large at early times. The normal test for the validity of the transport approximation is that the transport corrected results agree with those from a PN($N \geq 3$) expansion. From Figure 6, the transport approximation is in better agreement with the asymmetric P3 calculations than the consistent calculations in Figure 8.

5.4 ^{237}Np Results

The cross section for fission in ^{237}Np is considerably higher at high energies than at lower energies. As a result, the rate of decay of the fission rate is greater than for the ^{235}U case and experimental results are only available for about the first 60 channels (150 ns).

The comparisons between experiment and calculation show similar features to those for ^{235}U. Figure 9 shows that the asymmetric and transport corrected symmetric results are both low compared to the experiment for channels 20-60. The asymmetric calculations predict the peaks reasonably well, but the transport corrected results are high for low X and low for high X. Figure 10 summarises these comparisons. The consistent symmetric calculation agrees with the experiment at long times and with the transport corrected results near the peaks (Figure 11).

6. SUMMARY

The aim of the study was to find whether the differences observed between simple calculations and experiment were due to the simplifying assumptions with regard to the geometry of the experiment. The asymmetric calculations use a close representation of the experimental geometry and these calculations show the same, or possibly increased disagreement with the experiment. Thus, the observed differences are not due to effects of geometry but may be due to errors in the ^{232}Th cross sections or undetected errors in the calculations or experiments. Moo *et al.* have examined the changes required in the cross sections to bring about agreement between calculation and experiment. The good agreement between the consistent symmetric calculations and experiment is a further indication of the magnitude of the changes required in the total cross section, which would bring the calculations into agreement with the experiment.

7. ACKNOWLEDGEMENTS

I wish to thank Hugo Ferguson for preparing the data sets from the ENDF/B-III files and Michael Rainbow for running the FORFIT analysis of the calculations.

8. REFERENCES

Emmett, M.B. [1975] - The MORSE Monte Carlo radiation transport code system. ORNL-4972.

Inada, T., Kawachi, K. & Hiramoto, T. [1968] - *J. Nucl. Sci. Technol.*, 5:22.

Maher, K.J., Ritchie, A.I.M. & Rainbow, M.T. [1967] - Proc. IAEA Symp. on Neutron Thermalisation and Reactor Spectra, Vol. 2, p. 245.

Moo, S.P., Rainbow, M.T. & Ritchie, A.I.M. [1973] - Time-dependent ^{237}Np, ^{235}U and ^{239}Pu fission rates in a thorium assembly during the interval 0 to 200 ns using a pulsed $^{9}Be(d,n)$ source. Part I - experiment. AAEC/E254.

Moo, S.P., Rainbow, M.T. & Ritchie, A.I.M. [1974] - Time-dependent ^{237}Np, ^{235}U and ^{239}Pu fission rates in a thorium assembly during the interval 0 to 200 ns using a pulsed $^{9}Be(d,n)$ source. Part II - theory. AAEC/E295.

Wright, R.Q., Greene, N.M., Lucius, J.L. & Craven, C.W. Jr. [1969] - SUPERTOG: a program to generate fine group constants and P_n scattering matrices from ENDF/B. ORNL-TM-2679.

TABLE 1

GROUP-DEPENDENT QUANTITIES

Group	Top Energy	Spectrum N(E)dE	Macroscopic Cross Sections Total	Transport	Group	Top Energy	Spectrum N(E)dE	Macroscopic Cross Sections Total	Transport
1	1.00+7	0.001	0.1703	0.0985	22	4.98+5	0.009	0.2206	0.1713
2	7.79+6	0.025	0.1850	0.1043	23	4.51+5	0.009	0.2264	0.1796
3	6.07+6	0.120	0.2066	0.1128	24	4.08+5	0.009	0.2331	0.1886
4	4.72+6	0.158	0.2278	0.1209	25	3.69+5	0.010	0.2399	0.1976
5	3.68+6	0.109	0.2241	0.1252	26	3.34+5	0.010	0.2468	0.2069
6	2.87+6	0.094	0.2092	0.1287	27	3.02+5	0.006	0.2543	0.2166
7	2.23+6	0.040	0.2000	0.1303	28	2.73+5	0.006	0.2623	0.2266
8	2.02+6	0.040	0.1961	0.1302	29	2.47+5	0.005	0.2708	0.2371
9	1.83+6	0.037	0.1936	0.1299	30	2.24+5	0.005	0.2793	0.2477
10	1.65+6	0.034	0.1909	0.1295	31	2.02+5	0.005	0.2879	0.2581
11	1.50+6	0.034	0.1895	0.1318	32	1.83+5	0.012	0.3022	0.2759
12	1.35+6	0.026	0.1884	0.1358	33	1.43+5	0.009	0.3218	0.2999
13	1.23+6	0.026	0.1881	0.1360	34	1.11+5	0.007	0.3382	0.3201
14	1.11+6	0.023	0.1881	0.1349	35	8.65+4	0.006	0.3525	0.3378
15	1.00+6	0.020	0.1884	0.1359	36	6.74+4	0.004	0.3657	0.3540
16	9.07+5	0.020	0.1885	0.1378	37	5.25+4	0.003	0.3349	0.3269
17	8.21+5	0.015	0.1898	0.1399	38	4.09+4	0.003	0.3300	0.3241
18	7.43+5	0.015	0.1932	0.1434	39	3.18+4	0.002	0.3340	0.3297
19	6.72+5	0.013	0.1986	0.1478	40	2.48+4	0.002	0.3374	0.3340
20	6.08+5	0.011	0.2068	0.1539	41	1.93+4	0.001	0.3402	0.3378
21	5.50+5	0.011	0.2146	0.1628	42	1.50+4	0.001	0.3424	0.3410
					43-52		0		

NOTES

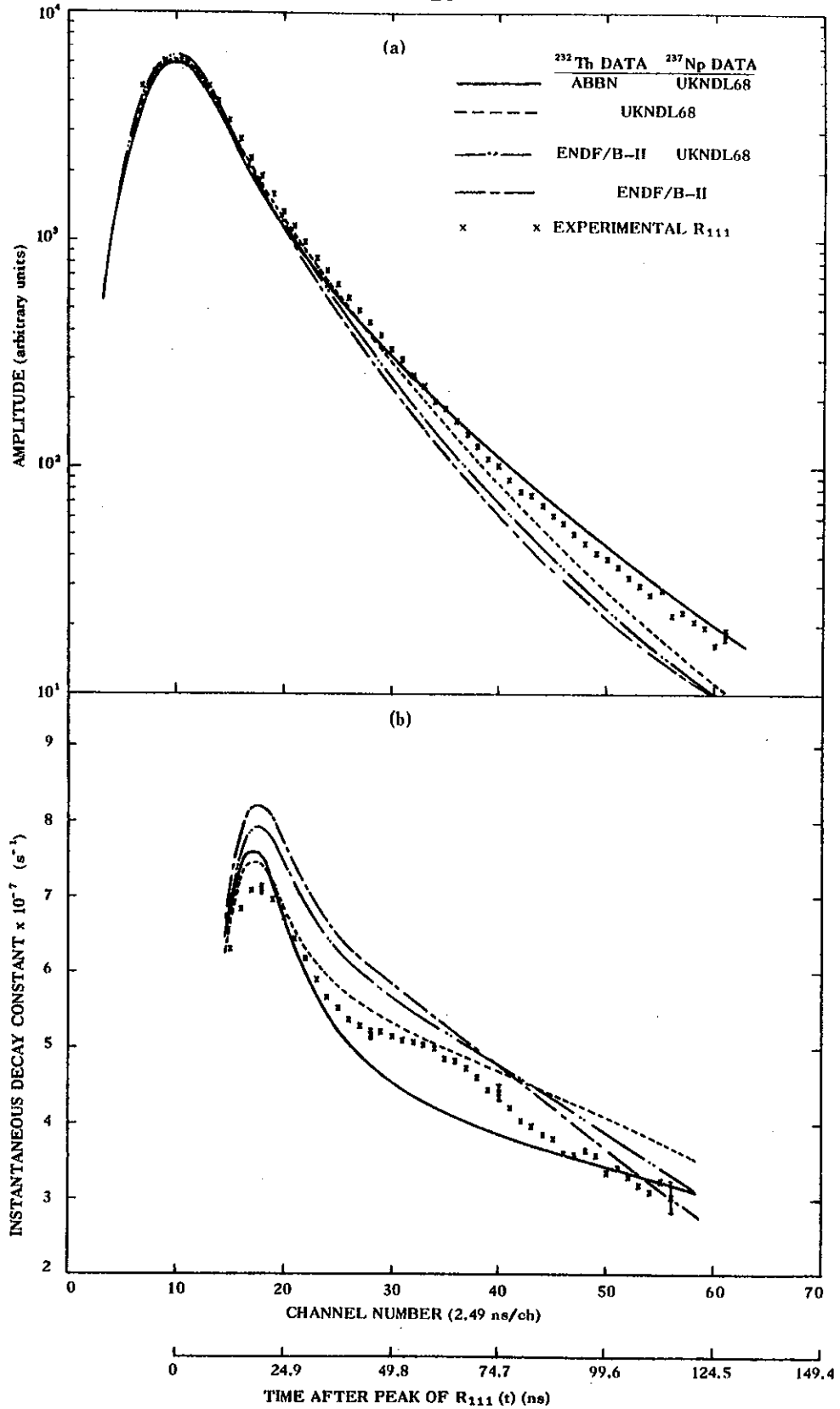

FIGURE 1. THEORETICAL AND EXPERIMENTAL VALUES OF THE FUNDAMENTAL MODE FISSION RATES FOR ^{237}Np AS A FUNCTION OF TIME (a) THE FUNDAMENTAL MODE TIME DISTRIBUTION (b) THE INSTANTANEOUS DECAY CONSTANT $\lambda(t)$ (After Moo et al., 1974)

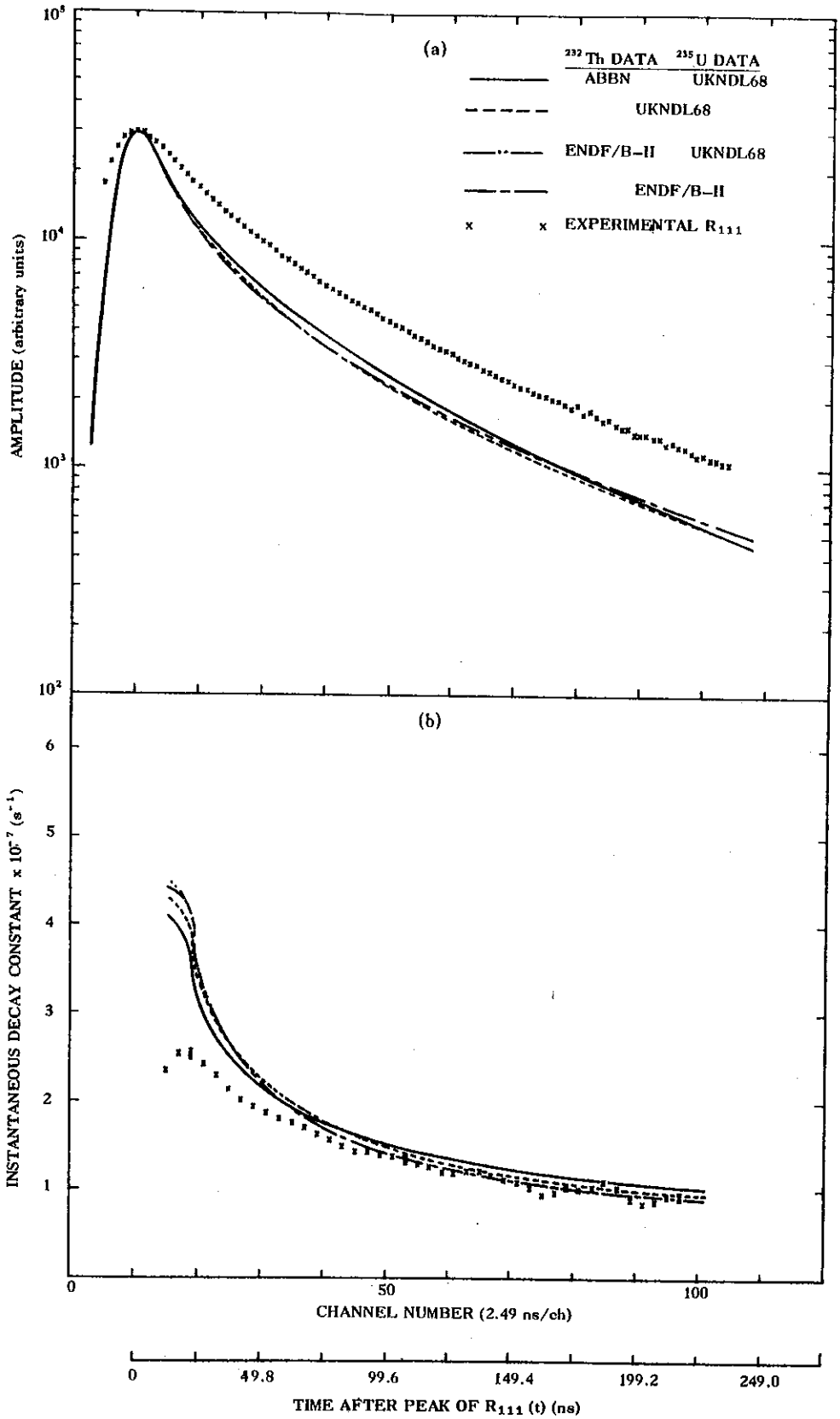

FIGURE 2. THEORETICAL AND EXPERIMENTAL VALUES OF THE FUNDAMENTAL MODE FISSION RATES FOR ^{235}U AS A FUNCTION OF TIME (a) THE FUNDAMENTAL MODE TIME DISTRIBUTION (b) THE INSTANTANEOUS DECAY CONSTANT $\lambda(t)$ (After Moo et al., 1974)

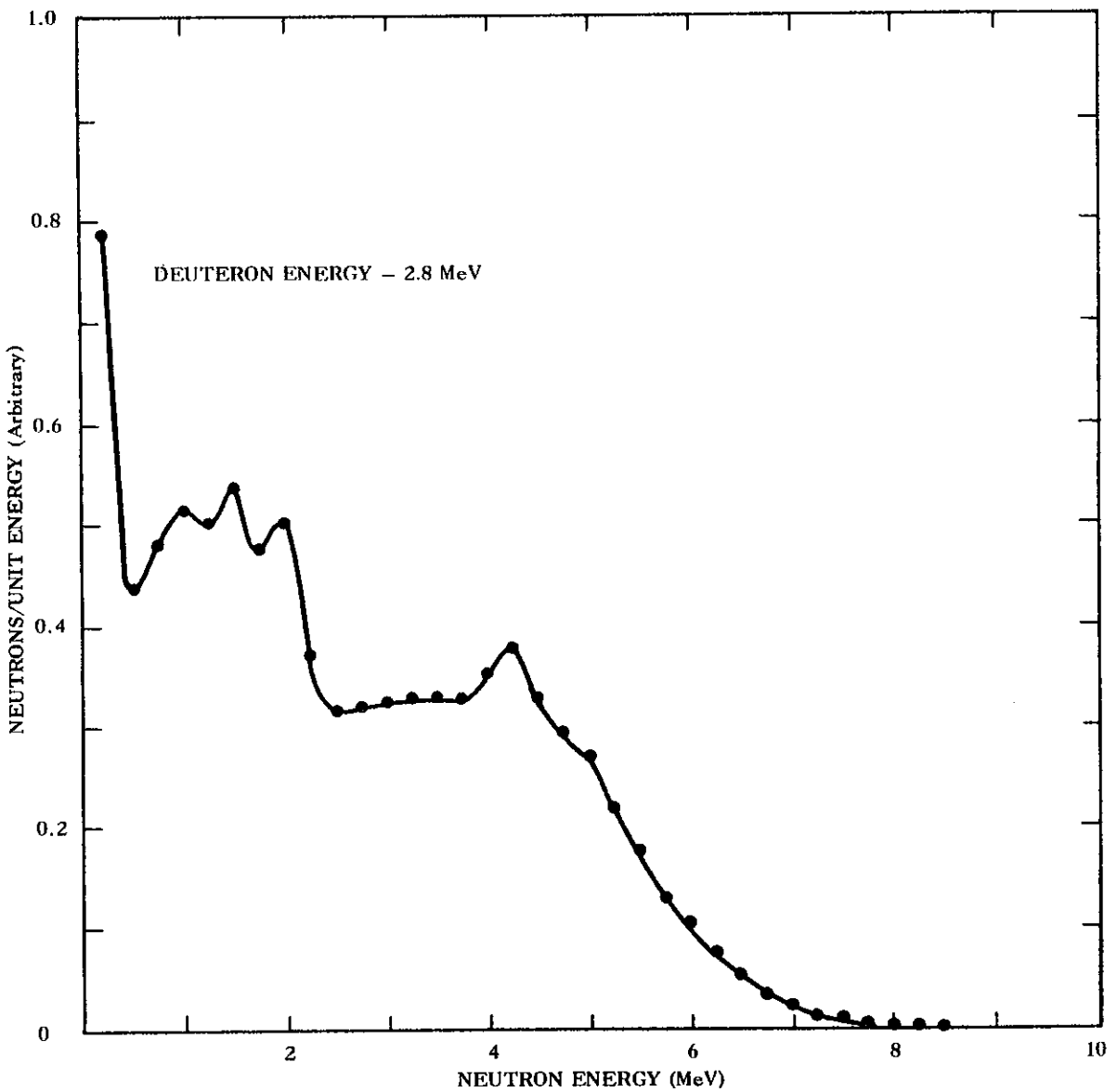

FIGURE 3. ANGLE-INTEGRATED NEUTRON ENERGY SPECTRUM FROM THE $^{9}Be(d,n)\,^{10}B$ THICK TARGET REACTION (After Moo et al., 1974)

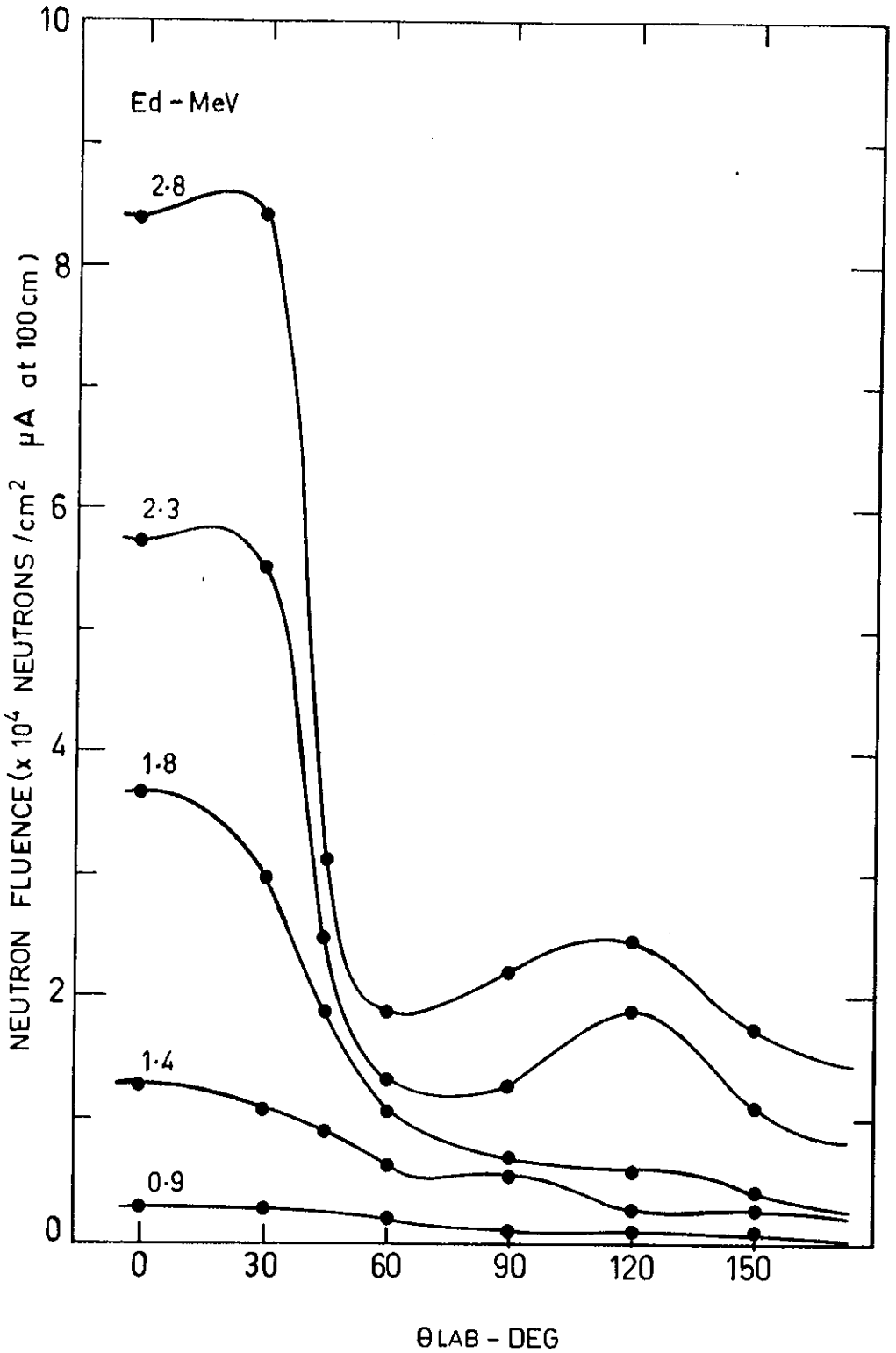

FIGURE 4. ANGULAR DISTRIBUTIONS OF FAST NEUTRON FLUENCE PRODUCED BY UNIT CURRENT OF DEUTERON BEAM INCIDENT ON A THICK Be DISK AT VARIOUS BOMBARDING ENERGIES (After Inada et al., (1968) J.Nucl. Sci. Technol. 5:22)

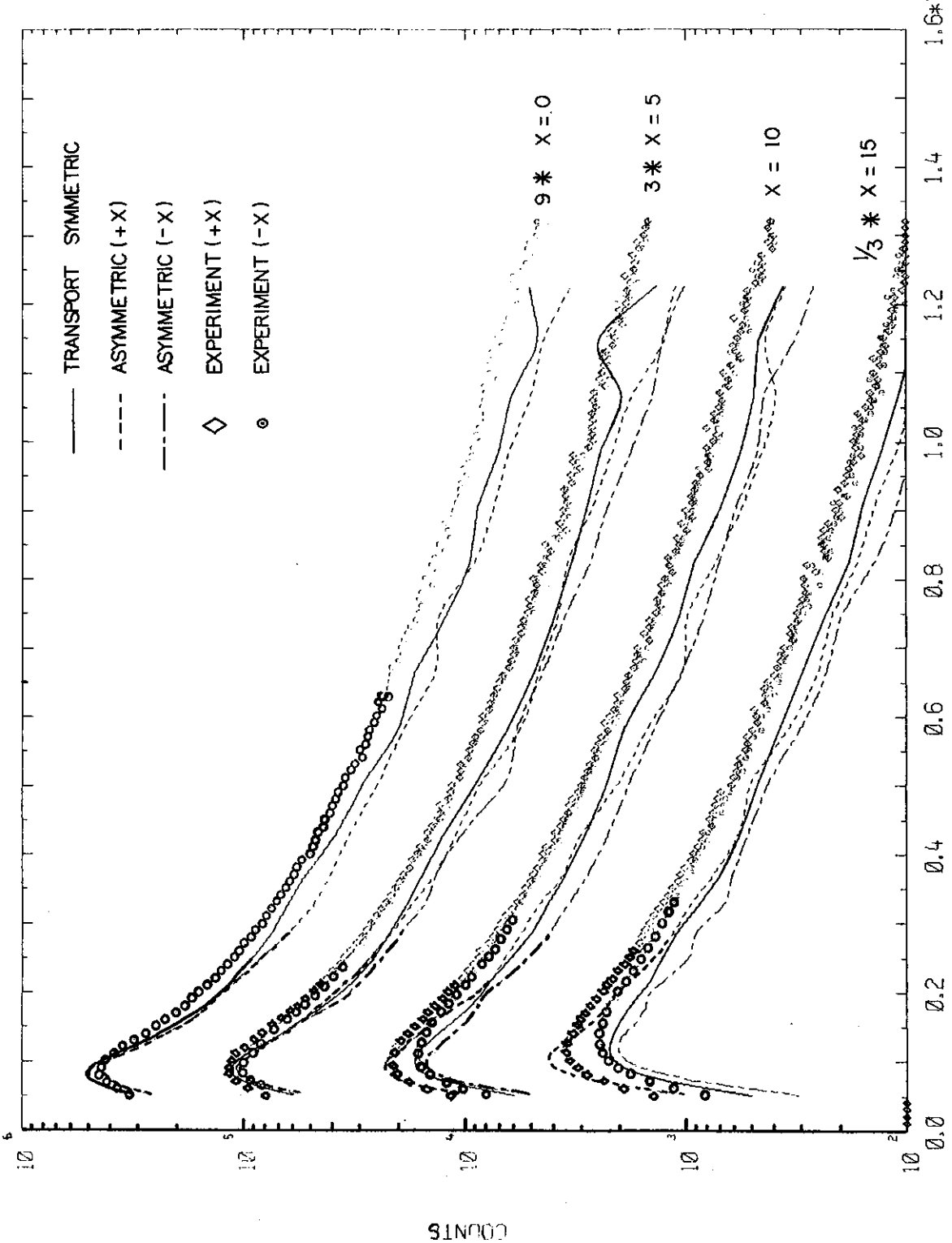

FIGURE 5. COMPARISON OF ASYMMETRIC AND TRANSPORT SYMMETRIC CALCULATIONS WITH EXPERIMENTAL 235U FISSION RATE AT 4 POSITIONS

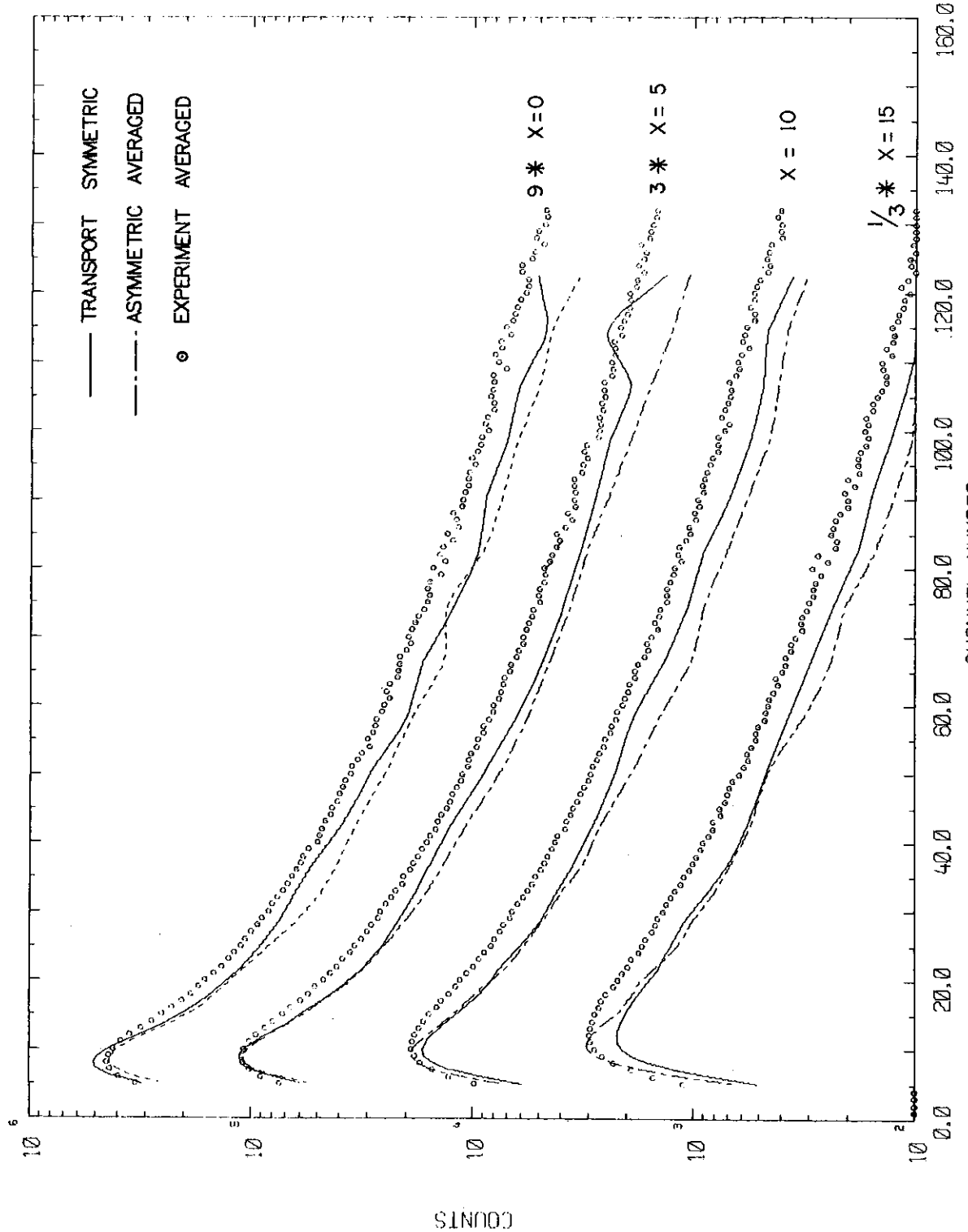

FIGURE 6. COMPARISON OF AVERAGED ASYMMETRIC AND TRANSPORT SYMMETRIC CALCULATIONS WITH AVERAGED EXPERIMENTAL 235U FISSION RATE AT 4 POSITIONS

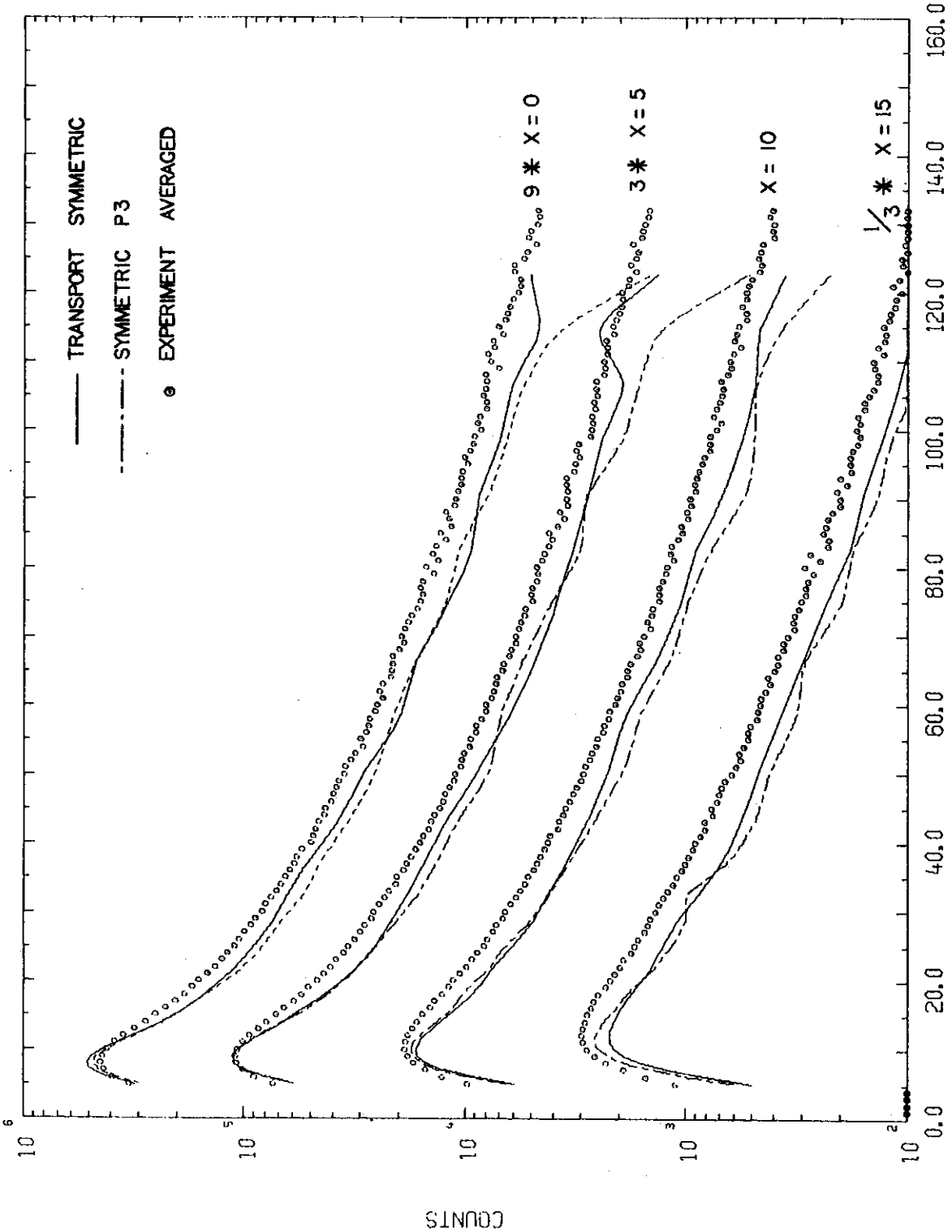

FIGURE 7. COMPARISON OF SYMMETRIC P3 AND TRANSPORT SYMMETRIC CALCULATIONS WITH AVERAGED EXPERIMENTAL 235U FISSION RATE AT 4 POSITIONS

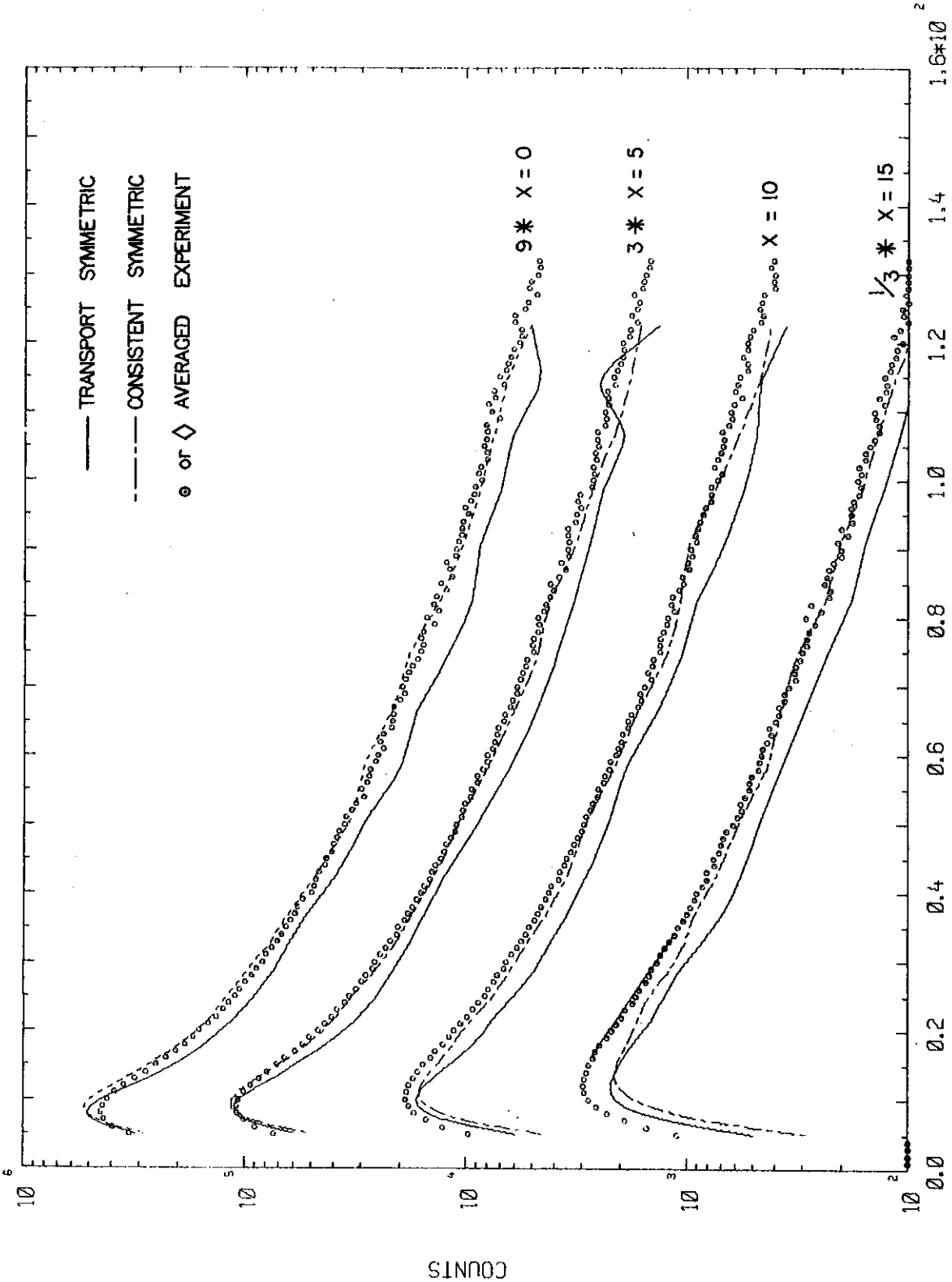

FIGURE 8. COMPARISON OF CONSISTENT AND TRANSPORT SYMMETRIC CALCULATIONS WITH AVERAGED EXPERIMENTAL ^{235}U FISSION RATE AT 4 POSITIONS

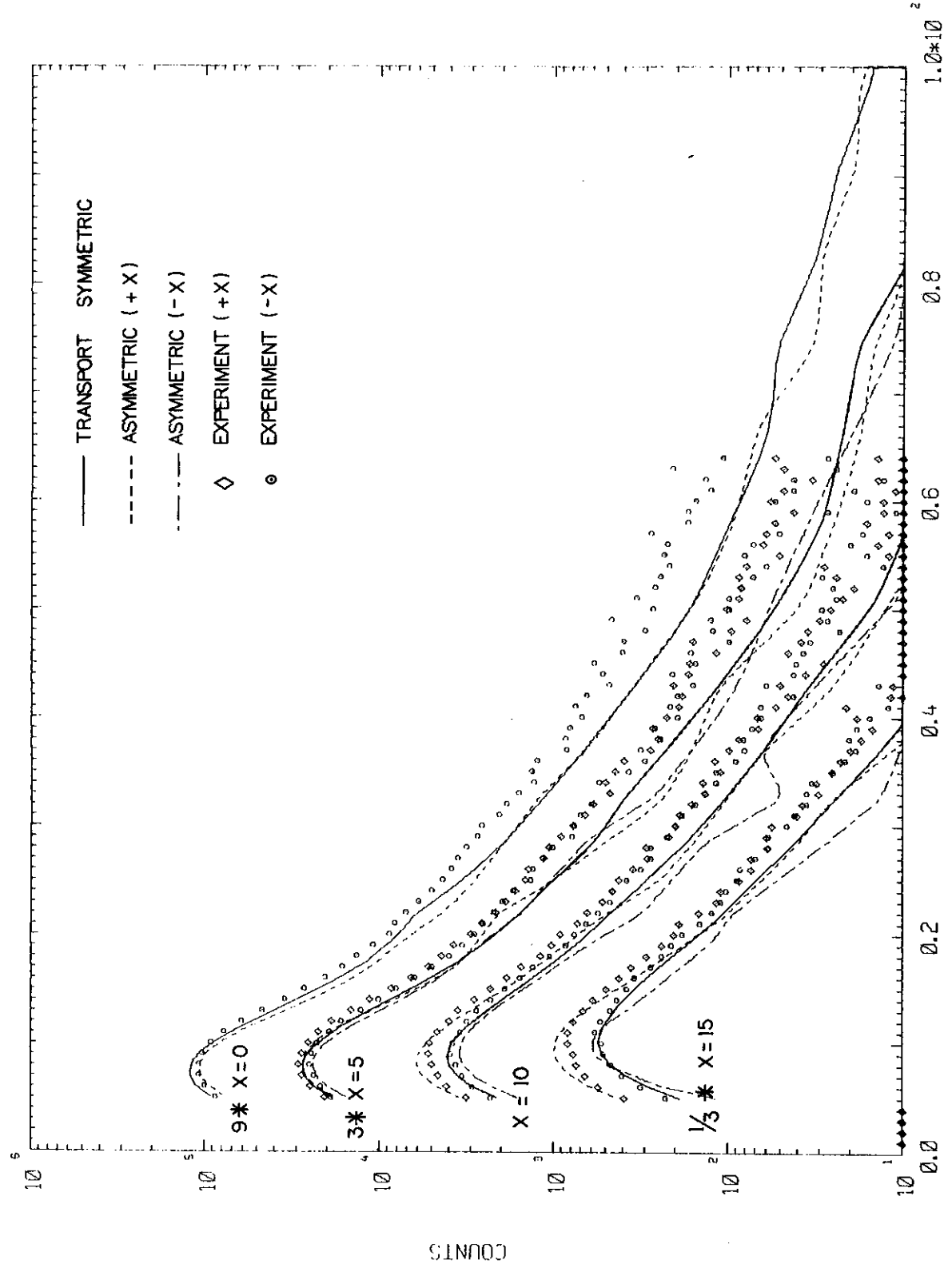

FIGURE 9. COMPARISON OF ASYMMETRIC AND TRANSPORT SYMMETRIC CALCULATIONS WITH EXPERIMENTAL ^{237}Np FISSION RATE AT 4 POSITIONS

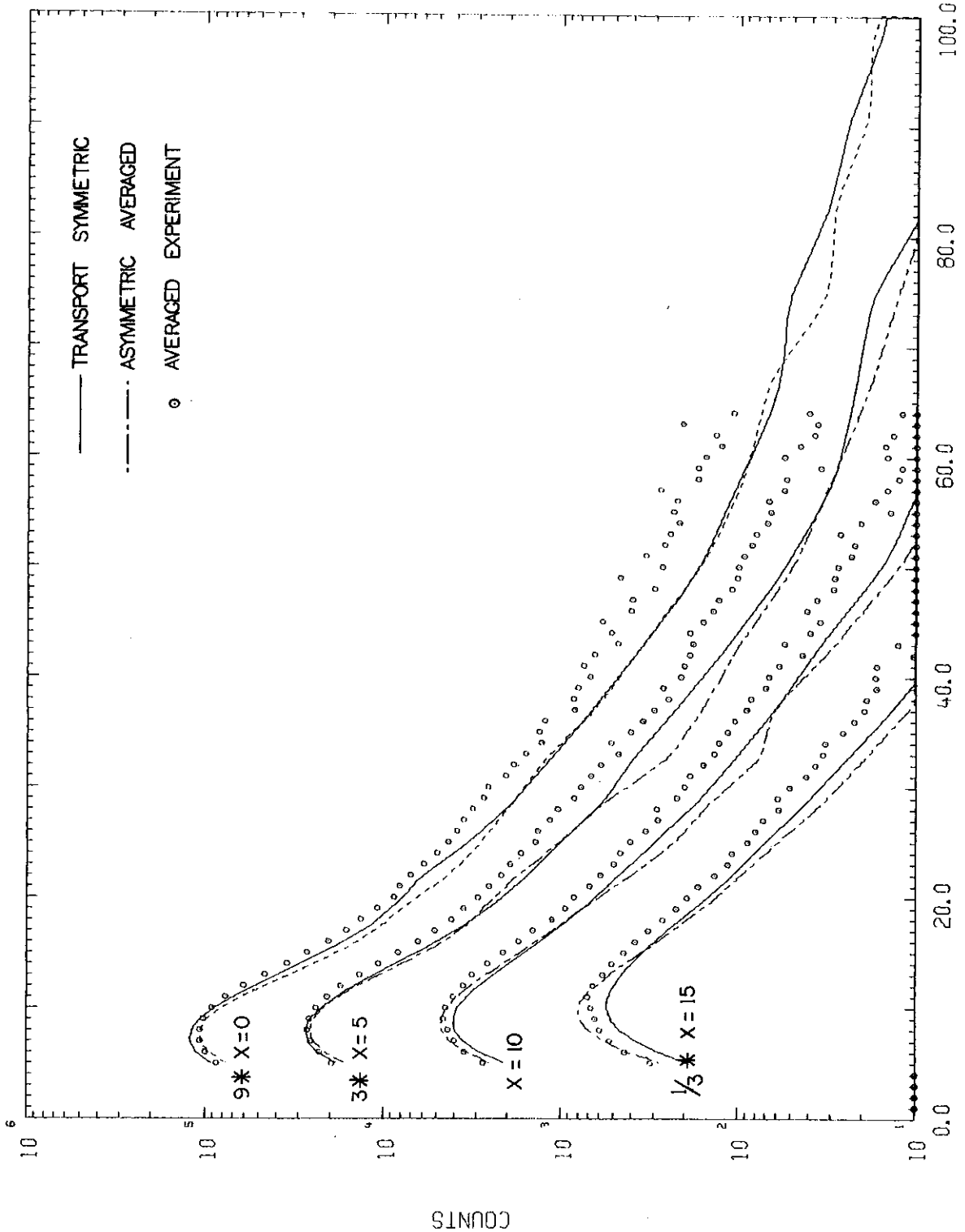

FIGURE 10. COMPARISON OF AVERAGED ASYMMETRIC AND TRANSPORT SYMMETRIC CALCULATIONS WITH AVERAGED EXPERIMENTAL ^{237}Np FISSION RATE AT 4 POSITIONS

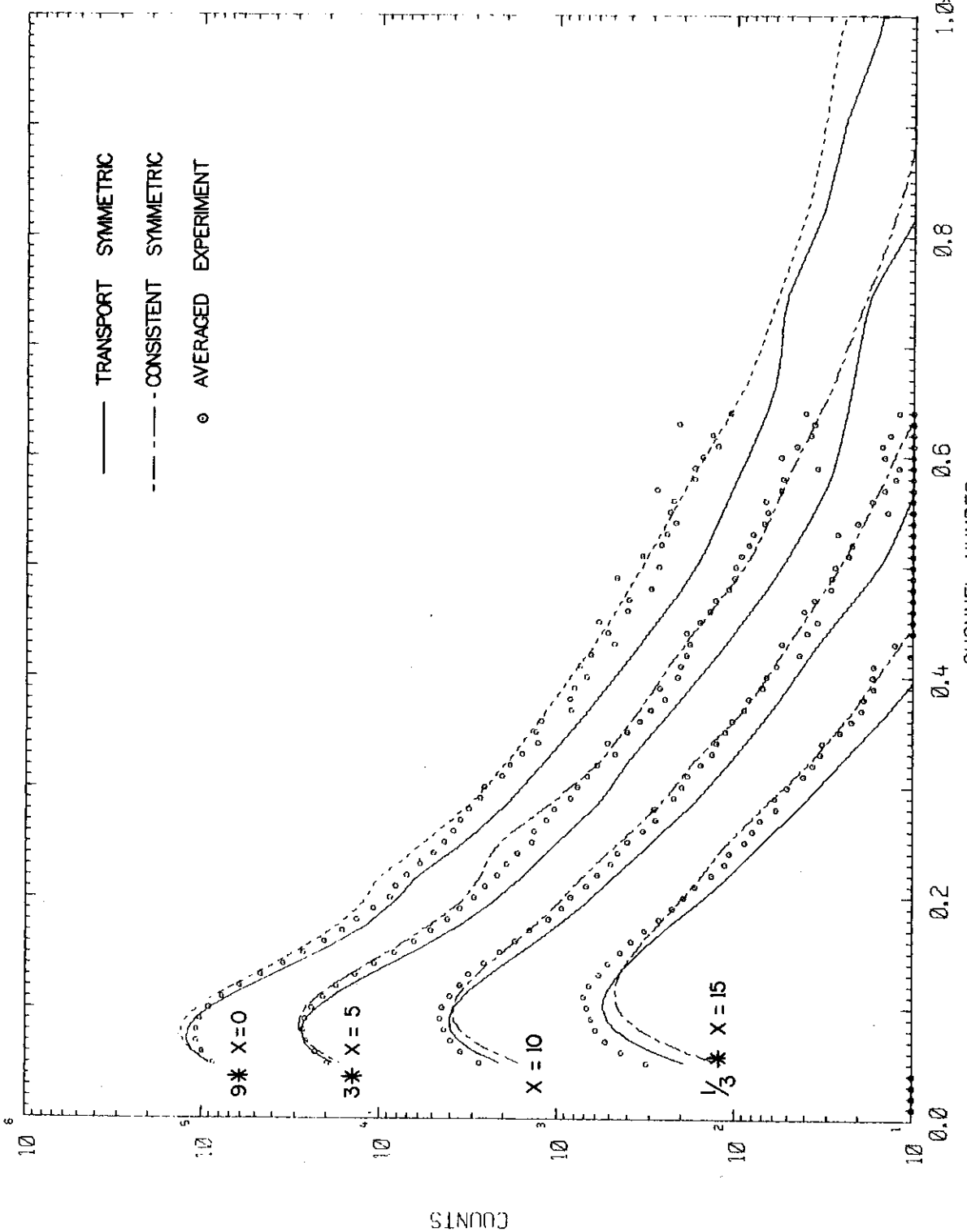

FIGURE 11. COMPARISON OF CONSISTENT AND TRANSPORT SYMMETRIC CALCULATIONS WITH AVERAGED EXPERIMENTAL ^{237}Np FISSION RATE AT 4 POSITIONS

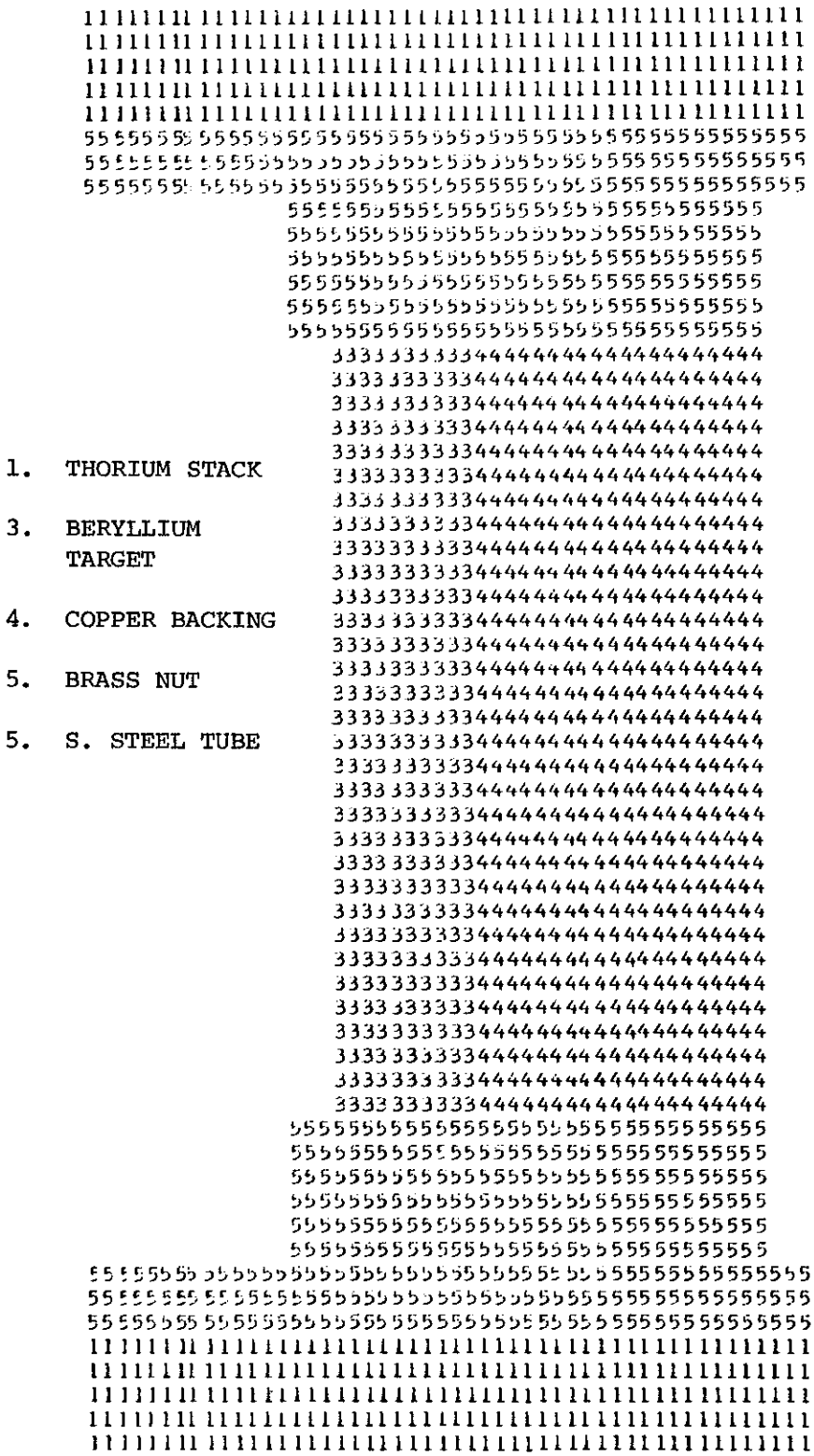

FIGURE 12. TARGET GEOMETRY